Photoelectron Spectroscopy on Thin Films of Extended Copper Porphyrazines

D. Pop,* B. Winter, W. Freyer, R. Weber, W. Widdra,† and I. V. Hertel

Max-Born-Institut für Nichtlineare Optik und Kurzzeitspektroskopie, Max-Born-Strasse 2A, D-12489 Berlin, Germany

Received: January 12, 2004; In Final Form: March 31, 2004

The present work is concerned with the interactions between a copper atom and an organic environment. We report photoemission spectra of the valence region and of the core levels for thin films of copper porphyrazine molecules with stepwise increased ligand size. The extension of the molecular ligand is obtained by linear benzoannelation. Specifically, the electronic structure and the metal-to-ligand and ligand-to-metal charge-transfer processes are investigated for the *t*-butyl substituted copper−tetraazaporphyrin, −phthalocyanine, −naphthalocyanine, and −anthracyanine using synchrotron as well as AlKα radiation. Information about charge-transfer processes is inferred as a function of the molecular π-electron system from the ratios between the copper satellites and the main lines, for both the Cu2p and the valence regions of the photoemission spectra. The experiments were performed at the MBI−BESSY undulator beamline at the synchrotron radiation facility BESSY II.

1. Introduction

The class of porphyrazine molecules has attracted considerable interest[1,2] based on their potential for technological and medical applications and on their similarity to natural porphyrins. These molecules, consisting of a central C_8N_8 ring with four pyrrole groups, are also remarkable due to their high symmetry, planarity, and electron delocalization.[3] The large family of porphyrazine compounds is generally understood to contain the tetraazaporphyrin (TAP or porphyrazine) and its analogues: phthalocyanine (Pc), naphthalocyanine (Nc), and anthracyanine (Ac). The porphyrazine macrocycle has high chemical versatility, which allows the electronic structure and properties to be tailored through modifications of the ligand and/or the central atom(s).[3,4]

This has spawned a whole area of technological applications and fields of scientific investigations. Tetraazaporphyrins have recently attracted interest for their nonlinear optical properties[5] and significant potential in molecular electronics.[6] Phthalocyanines are by far the most investigated porphyrazine molecules; they are chemically and thermally stable and sublime without decomposition. This makes them particularly attractive for the preparation of thin films by sublimation. Their field of application is large, including gas sensors, computer read/write disks, low-dimensional conductive materials, electrochromic devices, injection layers in organic light emitting devices (OLEDs), sensitizers for photodynamic therapy, liquid crystals, energy conversion (photovoltaic and solar cells), and nonlinear optics.[5,7,8] Also naphthalocyanines proved to be appreciable candidates for high-density optical recording media,[9] sensitizers for photomedicine,[10] and nonlinear optics,[5,11] as well as for synthesis of highly conductive, bridged polymers.[12] The greater conjugation of naphthalocyanines warrants improved electrical properties as compared to phthalocyanines. Although the first anthracyanine types of molecules were synthesized in 1971, the experiments performed on these systems are relatively scarce. Currently, they are investigated to obtain a new generation of photosensitizers for photodynamic therapy,[13] as well as for their potential in data storage.[14]

Considering the importance and versatility of these molecules, a detailed understanding of their electronic structure, charge transfer processes, and excited state dynamics is required. A suitable method for obtaining such information is photoelectron spectroscopy. In fact, tetraazaporphyrins have recently captured increased interest in photoemission studies. Theoretical investigations were aimed to determine the core level spectra for the copper containing molecules[15] and their valence density of states.[16] X-ray photoelectron spectroscopy (XPS) measurements, using monochromatized AlKα radiation, were performed on octaethylporphyrazine ($PzEt_8H_2$).[17]

A comprehensive overview on earlier photoemission studies of phthalocyanines is given in ref 18. Here, we just mention a few: the first photoemission work on a phthalocyanine molecule,[19] X-ray photoemission spectra of the valence region of H_2Pc and several metal phthalocyanine films,[20] HeI ultraviolet photoemission spectra of H_2Pc and MPc (M = Mg, Fe, Co, Ni, Cu, and Zn) in the gas phase,[21] and important investigations of the valence band electronic structure[22,23] and core levels[24] of phthalocyanines using synchrotron radiation. Recently, photoemission studies on newly synthesized phthalocyanine molecules have been published.[25]

Concerning naphthalocyanines, the first report of an X-ray photoemission spectrum was given in ref 26. As a general trend, the interest in the photoemission experiments was primarily focused on the investigation of C1s and N1s XP spectra of pure and oxygen doped naphthalocyanines.[27−29]

So far, no photoemission studies on anthracyanine molecules were reported. Also, there has been no systematic investigation of the effects of benzoannelation on the photoemission spectra of copper porphyrazines.

This paper reports photoemission studies from a system of copper porphyrazines with stepwise increased ligand size. We present and discuss the measured photoemission spectra of the

* Corresponding author. E-mail: dpop@mbi-berlin.de. Phone: 49-30-63921238. Fax: 49-30-63921229.

† Present address: Martin-Luther-Universität Halle-Wittenberg, D-06099 Halle, Germany.

10.1021/jp049850h CCC: $27.50
Published on Web 05/28/2004

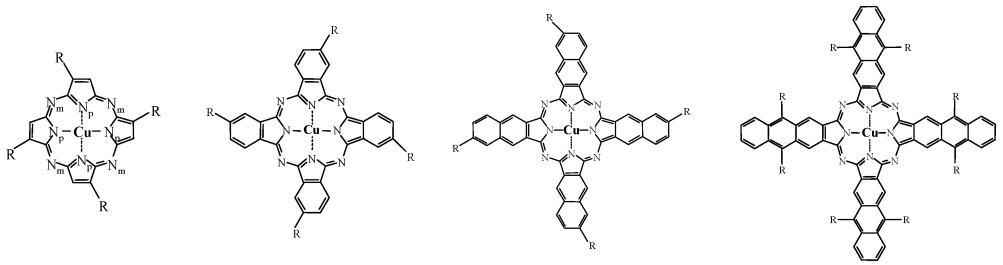

	CuP0	CuP1	CuP2	CuP3
λ_{max} [nm]:	585	677	770	878

R=$C(CH_3)_3$ for CuP0, CuP1, and CuP2
R=C_6H_5 for CuP3
R=H for CuTAP, CuPc, CuNc, and CuAc

Figure 1. Illustration of the copper porphyrazine molecules investigated in the present work. R denotes a substituent group, which is *t*-butyl for CuP0, CuP1, and CuP2 and phenyl for CuP3, respectively. The different characters of the nitrogen atoms in the molecules are marked only for the CuP0 molecule: N_p denotes a pyrrole nitrogen atom, and N_m denotes a meso-nitrogen atom. The characteristic absorption maxima for the compounds dissolved in benzene are given by λ_{max} (±1 nm uncertainty).

valence region and core levels for films of copper *t*-butyl substituted tetraazaporphyrin, phthalocyanine, naphthalocyanine, and anthracyanine. These investigations extend our previous studies on the corresponding metal-free compounds.[30] The satellites in the valence-region spectra of copper porphyrazine compounds are treated in a more complex and detailed manner than was previously done for related copper complexes. One key point is the analysis of the intensity variations of the copper satellite peaks in the photoemission spectra with the extension of the ligand size. This reveals information on the interaction between metal and ligand.

The main focus of the present work is on the electronic structure of *t*-butyl substituted copper porphyrazines and on charge-transfer processes (ligand-to-metal and metal-to-ligand) as a function of the size of the molecular π-electron system.

2. Experimental Procedures

2.1. Materials. The copper porphyrazine molecules studied here are sketched in Figure 1. Details as to the synthesis of the compounds were discussed in ref 31. The chemical names of the four molecules, from left to right in Figure 1 are copper tetra(*t*-butyl) porphyrazine, copper tetra(*t*-butylbenzo) porphyrazine (or copper tetra(*t*-butyl) phthalocyanine), copper tetra(*t*-butylnaphtho) porphyrazine (or copper tetra(*t*-butyl) naphthalocyanine), and copper octaphenyl-tetraanthraporphyrazine (or copper octaphenyl-anthracyanine), respectively. For simplicity, these molecules are denoted here as CuP0, CuP1, CuP2, and CuP3, where P is the symbol for porphyrazine, and the numbers 0, 1, 2, and 3 represent the number of benzo units fused to each pyrrole group. Their corresponding metal-free compounds (in which the central copper atom is replaced by two hydrogen atoms) will be referred to as H_2P0, H_2P1, H_2P2, and H_2P3. The molecules in Figure 1, in the absence of any *t*-butyl or phenyl substituent (symbolized by R), correspond to copper−tetraazaporphyrin (or porphyrazine) (CuTAP), −phthalocyanine (CuPc), −naphthalocyanine (CuNc), and −anthracyanine (CuAc). *t*-Butyl or phenyl substitution largely facilitates the synthesis and purification of materials; these substituents were found to insignificantly affect the optical absorption spectra. For CuPc, for example, the characteristic absorption maximum in the optical absorption spectra shows a shift of only 6 nm upon *t*-butyl substitution. The increase in the number of benzo units, however, causes a strong shift of the characteristic absorption maximum toward longer wavelengths, which is a consequence of the stronger delocalization of the molecular π-electron system.[31,32] The respective absorption maxima for the compounds dissolved in benzene are indicated by λ_{max} at the bottom of each molecule in Figure 1. For the respective unsubstituted CuPc molecule, the strong absorption is primarily attributed to the $a_{1u} \rightarrow e_g$ transition.[4,33] The a_{1u} is a pure ligand orbital, having the same composition as the HOMO of the metal-free molecule, while e_g represents the lowest unoccupied (degenerate) molecular orbital of the system. The assignment of the absorption bands is similar for the *t*-butyl substituted molecules.[34]

2.2. Thin Film Preparation and Photoemission Measurements. Thin films of CuP0, CuP1, and CuP2 as well as of CuPc (which was measured for reference), and the corresponding films of metal-free compounds H_2P0, H_2P1, and H_2P2, were prepared by sublimation on a Au(111) single crystal in ultrahigh vacuum (2×10^{-10} mbar base pressure). The material was evaporated from open quartz crucibles mounted at ca. 5 cm distance from the 10 mm diameter gold substrate. During deposition, the crystal was kept at room temperature. Prior to deposition, the gold substrate was cleaned by repeated cycles of Ar^+ sputtering and annealing to 750 °C. The Au(111) single crystal was mounted on a manipulator that allowed for sample rotation (azimuth, tilt, polar) and translation in front of the energy analyzer used for photoelectron detection. The sublimation temperatures for film preparation were 180, 380, 550, and 320 °C for CuP0, CuP1, CuP2, and CuPc, respectively. For H_2P0, H_2P1, and H_2P2, the sublimation temperatures for film preparation were 180, 350, and 500 °C. As CuP2 and H_2P2 are particularly susceptible to fragmentation during sublimation, the deposition times for those materials were kept below 20 min. The existence of only intact molecules in the films was confirmed by optical absorption measurements in solution: we compared the absorption spectrum of the native material in solution and that recovered by dissolving the material from a quartz plate on which the respective film was grown under identical preparation conditions. No differences in the absorption spectra were observed, which indicates that the deposited films contained no molecular fragments. As a solvent, we used benzene or toluene, and the absorption spectra were recorded between 260 and 1200 nm. In certain cases, we also used tetrahydrofuran as a solvent, with the absorption spectra then being measured between 200 and 1200 nm. In addition, for each

compound the residual material, left in the quartz oven after film preparation, was also examined by measuring its absorption spectrum in solution. These spectra also coincided with those of the native materials in solution.

The typical CuPc film thickness, as estimated from the deposition rate monitored by a quartz crystal microbalance, was about 400 ± 40 Å. The CuP0, CuP1, and CuP2 films were made to roughly contain an identical number of molecules, by scaling the monitored thickness to the respective molecular mass. Following the film preparation, the sample was transferred into the analysis chamber for photoemission measurements under ultrahigh vacuum conditions.

In the case of the CuP3 compound, the films produced by UHV sublimation did show traces of decomposition fragments, as was inferred from the absorption measurements. We therefore used for this material an alternative preparation technique, a wet chemical method, similar to the Langmuir−Blodget technique. Thus, the CuP3 compound was dissolved in toluene, and the resulting solution was placed in a recipient containing water. After toluene had evaporated, a layer of molecules was left on the water surface. A gold plated mica wafer was dipped into the solution and was then extracted very slowly so that molecules present at the water surface would stick to the plate, forming a film. The plate was then dried by heating it to about 100 °C at 10^{-1} mbar and kept in an Ar atmosphere until transfer into the UHV chamber for measurements. Repeating the procedure (i.e., on-top deposition), thicker films could be obtained. However, the thickness of the films produced by this method could not be quantitatively controlled. This is because the thickness of the molecular layer formed at the water surface strongly depends on the concentration of the dissolved compound in toluene.

The photoemission spectra of a CuP2 film obtained in this way and those of a CuP2 film prepared by sublimation in UHV turned out to be similar. Hence, this method was considered to be also suitable for preparing CuP3 films. H_2P3 films, however, were found to be unstable upon film preparation.

The photoemission measurements were performed at the MBI−BESSY beamline at the synchrotron radiation facility BESSY II. Details were given in ref 30. Briefly, the base pressure in the UHV chamber used for measurements was better than 2×10^{-10} mbar. Photoelectrons were detected in normal emission geometry with grazing light incidence (83° with respect to the surface normal) and at 1° acceptance angle, using a hemispherical electron energy analyzer EA 125, Omicron. The energy resolution of the spectrometer was typically 150 meV at 10 eV pass energy.

3. Results and Discussion

3.1. Effect of the *t*-Butyl Substituent on the Photoemission Spectra. Figure 2 shows photoemission spectra of thin films of CuP1 and unsubstituted CuPc, obtained for 70.7 eV excitation energy. To simplify the discussion, the peaks are labeled by capital letters. The spectra were normalized for the maximum intensity of feature H, and the energy scale shows the electron binding energies with respect to the vacuum level. For clarity, the spectra are vertically displaced with respect to each other (top CuPc and bottom CuP1), and additionally, in the lower panel the CuPc spectrum (dotted) is plotted on top of the CuP1 spectrum to emphasize the changes in the photoemission features due to *t*-butyl substitution. Similar to the case of metal-free compounds,[30] the *t*-butyl leads to an intensity increase of the photoemission signals at the position of feature G and in the 9.5−16 eV binding energy range. The peak binding energies

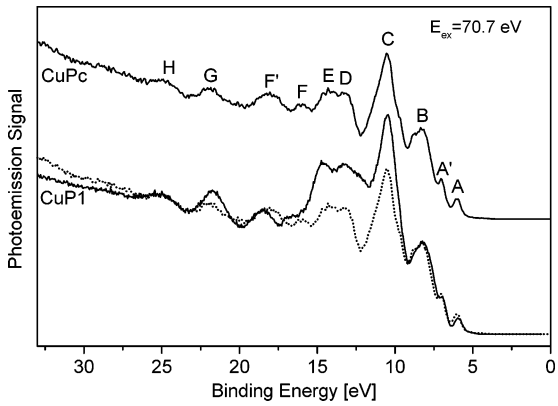

Figure 2. Photoemission spectra for unsubstituted CuPc (top−solid line and bottom−dotted line) and CuP1 (bottom−solid line) thin films at 70.7 eV photon energy. Electron binding energies are given with respect to the vacuum level. Intensities are normalized to the signal intensity of band H. Labels and their assignment are discussed in the text.

are generally identical for CuPc and CuP1. Exceptions are feature G, which is shifted by approximately 0.2 eV toward lower binding energies, and peaks E and F′, which are shifted by ∼0.3 and ∼0.4 eV, respectively, toward larger binding energies. Because of the *t*-butyl addition, band F is no longer resolved. The reason for the narrowing of band F′ in CuP1 as compared to CuPc is unclear.

We conclude that the differences between the photoemission spectra of *t*-butyl substituted versus unsubstituted copper porphyrazines are essentially add-on contributions from the substituent, with no major effect on the electronic structure of the bare macrocycle. It is noted that this is also the case for the metal-free compounds.[30] These results also agree with the measurements of the optical absorption spectra.

3.2. Peak Assignment and Metal Features in the Spectra. Recent theoretical calculations showed that in the ground state the HOMO in CuPc is singly occupied, having metal 3d character. Under D_{4h} symmetry, the HOMO is described as an antibonding Cu−pyrrole nitrogen (Cu−N_p) state having 44% $Cud_{x^2-y^2}$ character and 56% Pc b_{1g} character,[4] or 49% $Cud_{x^2-y^2}$ character and 51% N_p b_{1g} character.[33] The HOMO-1 is a pure macrocycle a_{1u} orbital having in fact the same composition as the HOMO of the metal-free phthalocyanine. In CuPc, the first ionization removes an electron from the phthalocyanine a_{1u} orbital, although b_{1g} lies about 0.5 eV higher.[4] The ionization from b_{1g} was calculated to require 0.71 eV more energy than the one from a_{1u} [4] (or 0.61 eV more in ref 33). The a_{1u} orbital is determined to have an ionization energy of 6.51 eV,[4] or 6.0 eV in ref 33. The HOMO-2 is an orbital that largely arises from the meso-bridging nitrogen atoms.[33] The next deeper orbitals are largely attributed to the ligand. The other copper d-like ionizations have energies that differ by 1.64−4.38 eV from the energy of b_{1g}.[33]

Also for copper tetraazaporphyrin (copper porphyrazine), the b_{1g} has been calculated to be the highest occupied level, with significant $Cud_{x^2-y^2}$ electron contribution of about 52%[35] (or 45% as determined in ref 16). In contrast to the CuPc case where the first ionization removes an electron from the a_{1u} orbital, in copper tetraazaporphyrin (CuTAP) the first ionization has been calculated to occur from the upper b_{1g} orbital.[36] This has been attributed to the larger gap between the b_{1g} and the a_{1u} orbitals in CuTAP than in CuPc.

Because for the metal-free naphthalocyanine the a_{1u} orbital is more destabilized than in phthalocyanine,[30,37] the gap between

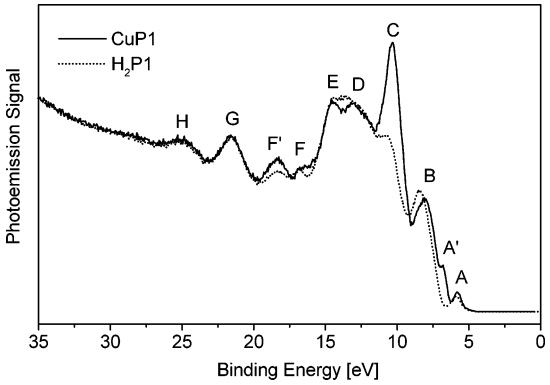

Figure 3. Photoemission spectrum of the CuP1 compound in comparison to the photoemission spectrum of the respective metal-free compound, H_2P1. The data were obtained for 70.7 eV photon energy.

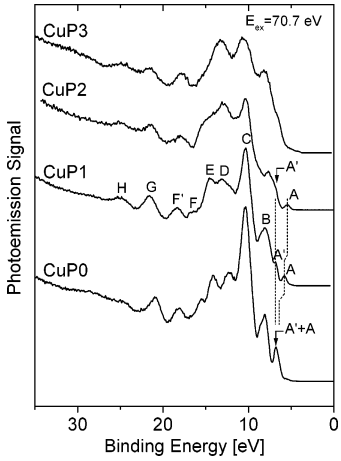

Figure 4. Photoemission spectra (vertically displaced with respect to each other) of the copper porphyrazines in the series; the ligand size increases from bottom to top. Spectra were obtained for 70.7 eV excitation energy. Electron binding energies are given with respect to the vacuum level.

the b_{1g} and the a_{1u} orbitals for CuNc is even smaller than for CuPc. Hence, in CuNc the first ionization must also occur from the a_{1u} orbital, similar to the CuPc case.

Figure 3 shows the photoemission spectra of the CuP1 compound and its corresponding metal-free complex, H_2P1. From the comparison of these two spectra, it appears that the spectrum of CuP1 can be regarded as the result of the mere addition of copper contributions to the metal-free H_2P1 spectrum. The comparison of the spectra in Figure 3 suggests that the features A, B, D, E, G, and H have ligand character while the features A′, C, F, and F′ contain, in addition to the ligand contributions, also the copper signal. On the basis of the previously mentioned theoretical reports,[4,33,36] of the assignment made for the H_2Pc spectrum,[18] of the comparison between H_2P1 and H_2Pc spectra,[30] and of the comparison between CuP1 and CuPc spectra, the photoemission features in Figure 3 can be assigned. Thus, feature A contains the signal from the a_{1u}-like orbital (which is the HOMO-1 in CuPc), while A′ contains emission from the b_{1g}-like orbital (which is the HOMO). The other features with mostly ligand character in the CuP1 spectrum include the following contributions: feature B: meso-nitrogen and benzene π; features D and G: benzene and *t*-butyl; feature E: 2p signal from the C and N atoms in the central ring and *t*-butyl; and feature H: benzene contributions. At the position of band C, in addition to the benzene and nitrogen contributions (and *t*-butyl for the substituted molecules), a strong copper d-like emission is found.[38] The bands F and F′ include Cu satellite signals in addition to the ligand emission.

3.3. Evolution of the Photoemission Features as a Function of the Ligand Size. The spectra for all Cu compounds in the series are displayed in Figure 4 for 70.7 eV excitation energy. Because the CuP3 film was obtained by a wet chemical method, its spectrum is less resolved than for the sublimed films, which is an indicative of poorer film quality. Moreover, the CuP3 spectrum is more difficult to interpret as this molecule contains phenyl rather than *t*-butyl as a substituent, and in addition, the corresponding metal-free spectrum is not available.

As expected, the intensity of the features containing benzene contributions increases considerably relative to the Cu3d main peak with extending the ligand size. Within the experimental accuracy, the binding energies of the Cu3d main peak (peak C) are identical for the CuP0, CuP1, and CuP2 compounds. Peak C is considerably broader for CuP3, most probably due to the additional ligand signal and also due to the preparation method. For CuP3, the copper emission can be hardly distinguished from ligand contributions.

The assignment of the photoemission features for CuP0, CuP2, and CuP3 is based on the results for CuP1 taking into account the chemical structure of the different molecules (CuP0 has no benzene moieties, and CuP3 has phenyl rather than *t*-butyl as substituent). Concerning the evolution of the ligand peaks, one observes in Figure 4 that bands H and G have the same binding energy for CuP1, CuP2, and CuP3, which is explained by the fact that they mainly arise from benzene units (and *t*-butyl for band G in CuP1 and CuP2). For CuP0, similarly to the metal-free complexes,[30] band H is considerably less pronounced, and band G is shifted by approximately 0.65 eV toward lower binding energies. Band D is found at the same position for CuP1 and CuP2, but it appears at a lower binding energy (by ∼0.4 eV) in CuP0. Again, this is consistent with a significant benzene character of this band for CuP1 and CuP2. Similar to the metal-free compounds case, band B does not shift upon the addition of benzo units for CuP0 and CuP1, most probably due to its large meso-nitrogen contributions. The peak position is found at slightly lower binding energy for CuP2.

For the discussion of the evolution of features A and A′ as a function of the ligand size, we will consider only the spectra of CuP0, CuP1, and CuP2 compounds since in the CuP3 spectrum these bands are not resolved. At about the binding energy of peak A′ in the CuP1 spectrum, a shoulder is present in the CuP2 spectrum. Because for the CuP1 compound the feature A′ contains the signal from the HOMO, we propose that this shoulder A′ in the CuP2 spectrum is derived from the HOMO of CuP2. Apparently, this feature is not better distinguishable because it strongly overlaps with ligand features. In CuP2, the binding energy of feature A is 5.48 ± 0.1 eV. Fitting the near edge valence region of the CuP1 spectrum by a sum of Gaussians, a binding energy of 5.78 ± 0.15 eV for peak A (derived from the a_{1u} ligand orbital) and 6.73 ± 0.15 eV for peak A′ (derived from the HOMO−b_{1g} orbital) is inferred. For the CuP0 compound, feature A is not resolved. The analysis of the band found at about 6.8 eV binding energy in the CuP0 spectrum reveals an asymmetric shape of this feature, with a low binding energy tail. Considering also that the a_{1u} derived peak is well-resolved for H_2P0,[30] we conclude that the asymmetric feature observed at ∼6.8 eV binding energy in the CuP0 spectrum includes both the HOMO (with partial metal character) and the HOMO-1 (with entire ligand character) photoemission signals. To determine the A and A′ contributions in the CuP0 spectrum, the near edge valence region was fitted by a sum of Gaussians. The width of the peak originating from the a_{1u} orbital

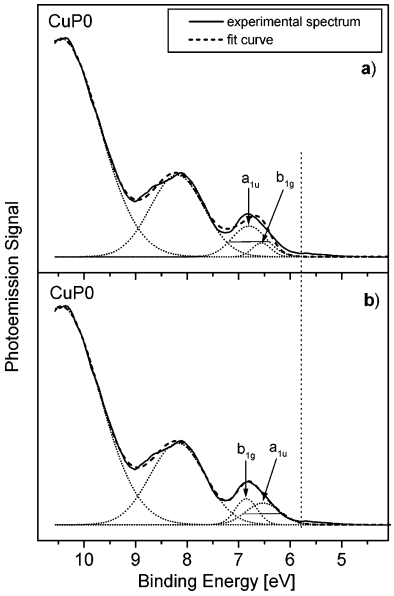

Figure 5. Peak fitting for the near-edge valence region of the CuP0 spectrum. (a) Fit performed assuming that the lowest binding energy peak originates from the HOMO-b_{1g} orbital with metal character. (b) Fit performed considering that, as for copper phthalocyanine, the peak of lowest binding energy originates from the a_{1u} orbital, having pure ligand character. The vertical dotted line indicates the binding energy determined for the peak derived from the a_{1u} molecular orbital in CuP1, namely, 5.78 eV.

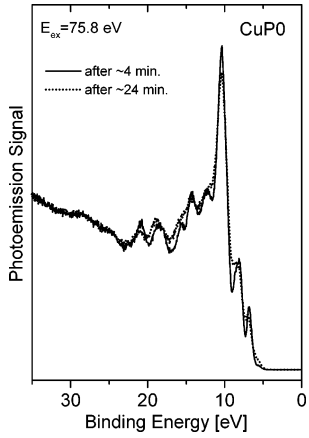

Figure 6. Photoemission spectra of a CuP0 thin film, measured on an identical surface spot after two different exposure times to synchrotron radiation.

TABLE 1: Binding Energies of the Peaks Derived from the a_{1u} and b_{1g} Orbitals in the Photoemission Spectra of CuP0, CuP1, and CuP2 Compounds

compound	binding energy of the b_{1g} orbital [eV]	binding energy of the a_{1u} orbital [eV]
CuP0	6.85	6.53
CuP1	6.73	5.78
CuP2	shoulder ~6.73	5.48

was imposed as a fixed fit parameter, the a_{1u} peak width being considered the same as in the H_2P0 spectra reported in ref 30. This is because the atomic contributions to the a_{1u} molecular orbital should be identical in CuP0 and H_2P0 (they are identical in CuPc and H_2Pc[4,33]). With this condition, the fit was performed in two ways. First, it was supposed that, in contrast to the case of CuP1 or CuPc, the peak derived from the HOMO has the smallest binding energy (see Figure 5a). This is in accordance with the theoretical results from ref 36 for the similar yet unsubstituted CuTAP compound, which claim that the first ionization removes an electron from the HOMO b_{1g} orbital and not from the HOMO-1 a_{1u} orbital, as for CuPc. The binding energies obtained with this fit are 6.56 ± 0.15 eV for the b_{1g} orbital and 6.80 ± 0.15 eV for the ligand a_{1u} orbital. For a second fit, it was supposed that similarly to the case of the CuP1 and CuP2 compounds, the peak with the lowest binding energy originates from the ligand a_{1u} orbital, and the peak with the next higher binding energy originates from the HOMO b_{1g} orbital (see Figure 5b). The binding energies thus obtained are 6.53 ± 0.15 eV for the a_{1u} orbital and 6.85 ± 0.15 eV for the b_{1g} orbital. One can observe that the fit in Figure 5a matches rather poorly the CuP0 experimental data, while the one in Figure 5b is of considerably improved quality. With the fit from Figure 5a, the separation between the a_{1u} derived peaks in CuP0 and CuP1 is 1.02 eV, whereas this is 0.75 eV in Figure 5b. Since the atomic contributions to the a_{1u} orbital are the same in the copper compounds and their similar metal-free complexes,[4] the difference between the binding energies of the peak derived from the ligand a_{1u} orbital in CuP0 and CuP1 should be similar to the difference between the binding energies of this peak in H_2P0 and H_2P1 (which is 0.67 eV[30]). We found this behavior also for the respective zinc-containing molecules.[39] Regarding this observation, the data obtained with the fit in Figure 5b are more consistent with the data for the metal-free compounds. Notice also that the separation between the peaks originating from the ligand a_{1u} orbital in CuP1 and CuP2 is 0.3 eV, which is in very good agreement with the separation found between the peaks derived from the ligand a_{1u} orbital in H_2P1 and H_2P2 (0.29 eV).[30] On the basis of all these arguments, we propose that the appropriate fit for CuP0 is the one in Figure 5b. Hence, we conclude that, like for CuP1 or CuPc, also for CuP0 the first ionization occurs from the ligand a_{1u} orbital. Table 1 summarizes the binding energies of the peaks derived from the a_{1u} and b_{1g} orbitals in the photoemission spectra of CuP0, CuP1, and CuP2 compounds.

The results presented here suggest that for *t*-butyl substituted copper−tetraazaporphyrin (CuP0), −phthalocyanine (CuP1), and −naphthalocyanine (CuP2), the first ionization does occur in all cases from the ligand a_{1u}-like orbital and not from the HOMO b_{1g}-like orbital. This is in agreement with the calculations for CuPc[4] and in contrast to theoretical results for CuTAP.[36] Thus, the peak of lowest binding energy in these spectra is comprised of a ligand signal. In going from a given molecule to the next larger one in the series, the shift of the a_{1u} photoemission feature is largest between CuP1 and CuP0. This confirms that the interactions induced by the benzene moieties, which determine the destabilization of the a_{1u} orbital, are stronger for the inner ring of benzo units directly surrounding the porphyrazine core and become weaker for the outer rings.[37]

3.4. Photostability. As in other synchrotron radiation studies, the radiation-induced damage of the organic films needs to be considered. Similar to the situation for the metal-free complexes,[30] the smallest molecule, CuP0, is the most sensitive one to synchrotron radiation exposure. The respective photoemission spectra exhibit changes even upon recording a spectrum. Figure 6 displays photoemission spectra obtained for different exposure times to 75.8 eV photons. Photodegradation leads to a broadening and a smearing out of all peaks. For CuP1, the effect of synchrotron light is less pronounced, and the photodegradation rate is considerably lower as compared to CuP0. Even smaller synchrotron radiation exposure effects are observed for the CuP2 compound. In this case, the main changes appear in the region

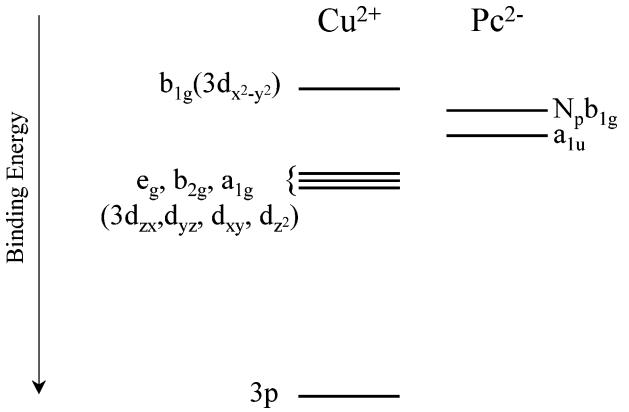

Figure 7. Scheme of the energy levels for Cu^{2+} and Pc^{2-} dianion in CuPc, which are relevant for this work.

of bands A, B, C, and G. No photodegradation effects were detected for the CuP3 films. As a consequence, for the present photoemission measurements, the irradiated spots on the sample were frequently changed.

3.5. Copper Satellites. The features between ~15.5 and ~19.5 eV binding energy (F and F′) in Figure 4 are assigned to copper satellites. In previous work on Cu-phthalocyanine (CuPc)[38], a $3d^84s^2$ final configuration of Cu was attributed to these satellites, based on the assumption that Cu in CuPc can be treated as quasiatomic. To the best of our knowledge, no other studies on the Cu valence satellites in CuPc or another copper porphyrazines have been reported ever since.

XAS (X-ray absorption spectroscopy) measurements proved that copper in CuPc is in a Cu^{2+} ionization state.[40] In compounds containing divalent copper ($3d^9$ formal configuration, e.g., copper dihalides[41] and CuO[42]), the ground-state configuration is considered to be a mix of $3d^9$ and $3d^{10}\underline{L}$, where $\underline{L}$ denotes a hole in the ligand. Thus, the final configurations attributed to the main line and the satellite in the valence band are $3d^9\underline{L} + 3d^{10}\underline{L}^2$ and $3d^8$, respectively.[41−44] However, the Cu2p satellites in CuPc were subject of several experimental[45,46] and theoretical studies,[15] and analogies were made to copper dihalides or CuO.

The presence of the satellites on the high-binding energy side of the main lines for the photoionization from Cu2p, Cu3s, or Cu3p levels of dihalides has been explained by the existence of two final states. One of them corresponds to a well-screened final state (main line) with the final configuration $\underline{c}3d^{10}\underline{L}$, when upon photoionization the unfilled 3d orbital is pulled down below the ligand level, and charge transfer from the ligand L to the copper 3d states occurs. The other one is an unscreened final state (satellite) with a final $\underline{c}3d^9$ configuration, when no charge transfer occurs upon photoionization.[41,47] Here, $\underline{c}$ and $\underline{L}$ indicate that there is a hole in the copper c core level and in the ligand L valence state, respectively. The central Cu atom in CuPc is formally divalent, and its site has D_{4h} symmetry, as in the case of copper dihalides. Thus, the interpretation of the main lines and of the satellites in the photoemission spectra of CuPc is analogous to that of copper dihalide compounds.

In the following, the physical processes governing the appearance of satellites and main lines in the valence and core level regions for CuPc will be discussed, referring to the relevant energy levels. The energy level diagram can be regarded as being composed of the bare macrocycle Pc^{2-} levels interspersed with the Cu^{2+} ones, as shown in Figure 7. For Cu compounds with a nominal $3d^9$ ground state configuration, the ligand p level is usually deeper than the Cu3d orbital having a valence hole.[45] In CuPc, the $Cud_{x^2-y^2}$ orbital has a single occupancy, and the ligand N_p b_{1g} level is the HOMO of the Pc^{2-} dianion.[33] The a_{1u} ligand macrocycle orbital and the other Cu3d orbitals are found even deeper.

As shown previously, according to theoretical calculations, the emission from the HOMO of CuPc/CuP1 (b_{1g} molecular orbital having $Cud_{x^2-y^2}$ and N_p character) gives rise to contributions at the position of feature A′ in the photoemission spectra. Because of its low binding energy, we suggest that this corresponds to a screened final state of copper. We propose that upon ionization, charge is transferred from the ligand (N_p b_{1g} level) to the $Cud_{x^2-y^2}$ orbital. This appears more likely than a two-hole $Cud_{x^2-y^2}$ state. Thus, the current picture is that part of feature A′ corresponds to a final state with one hole in the $Cud_{x^2-y^2}$ orbital and another hole in the ligand (N_p).

We conclude that at the other copper d-like ionizations, from $e_g(d_{zx},d_{yz})$, $b_{2g}(d_{xy})$, or $a_{1g}(d_{z^2})$ orbitals, the screening by electron transfer from the ligand N_p b_{1g} orbital into the $Cud_{x^2-y^2}$ orbital gives rise to the features observed at the position of band C in the spectra. This corresponds to a final configuration that has one hole in one of the previously mentioned d orbitals and a hole in the ligand ($Cud_{x^2-y^2}$ is filled by charge transfer). The satellite features correspond to the case when no charge transfer occurs upon ionization, and the final state has one hole in one of the e_g, b_{2g}, or a_{1g} orbitals and one hole in $Cud_{x^2-y^2}$ orbital. Consequently, the satellite features observed in the valence region of CuPc correspond to a Cu $3d^8$ final configuration.

The spectra of the *t*-butyl substituted Cu−porphyrazines, obtained for 75.8 and 70.7 eV photon energy, are presented in Figure 8. Arrows mark the positions of the Cu satellite peaks. Near 75 eV excitation energy, an increase of the Cu satellite intensity is observed for CuPc, CuP0, CuP1, and CuP2. The effect does not appear for CuP3. As for other divalent copper compounds, the satellite enhancement at about 75 eV photon energy is related to the 3p−3d transition in Cu, more precisely, to the transition from one of the 3p orbitals into the $Cud_{x^2-y^2}$ orbital. In the current picture, the $Cu3p-Cud_{x^2-y^2}$ excitation is accompanied by an Auger decay from one of the d-like $e_g(d_{zx},d_{yz})$, $b_{2g}(d_{xy})$, or $a_{1g}(d_{z^2})$ copper orbitals, with emission of a $Cud_{x^2-y^2}$ electron. Consequently, the final configuration reached for resonant excitation is $3d^8$, with one hole in one of the d-like $e_g(d_{zx},d_{yz})$, $b_{2g}(d_{xy})$, or $a_{1g}(d_{z^2})$ copper orbitals and one hole in $Cud_{x^2-y^2}$, which is the final configuration of the Cu valence satellite. Notice that the same configuration is obtained if the $Cu3p-Cud_{x^2-y^2}$ excitation is accompanied by the Auger decay of an electron from $Cud_{x^2-y^2}$, with emission of one electron from the $e_g(d_{zx},d_{yz})$, $b_{2g}(d_{xy})$, or $a_{1g}(d_{z^2})$ orbitals. We conclude that these mechanisms lead to the enhancement of the satellite features from the valence region when the condition for $Cu3p-Cud_{x^2-y^2}$ excitation is fulfilled. As for other compounds containing divalent copper,[43,48] around 75 eV photon energy, the direct photoemission is in resonance with the Auger electron emission, and their coherent superposition can occur.

Figure 9 shows the intensity change in the region of Cu satellite peaks (at the position of bands F and F′) as a function of photon energy for CuP0. The intensity changes were obtained by integrating the spectrum at the position of bands F and F′ and normalization to the intensity on the high binding energy side of feature G. The intensity change exhibits a double-peak structure. A similar dependence is also obtained for CuP1, CuP2, and CuPc. In all cases, these data may be well fitted by a superposition of two Gaussians of equal widths, separated by 2.2 eV. This spacing corresponds to the $Cu3p_{1/2}-Cu3p_{3/2}$ splitting; therefore, the two-peak structure is attributed to the excitation from the spin−orbit split Cu3p components.

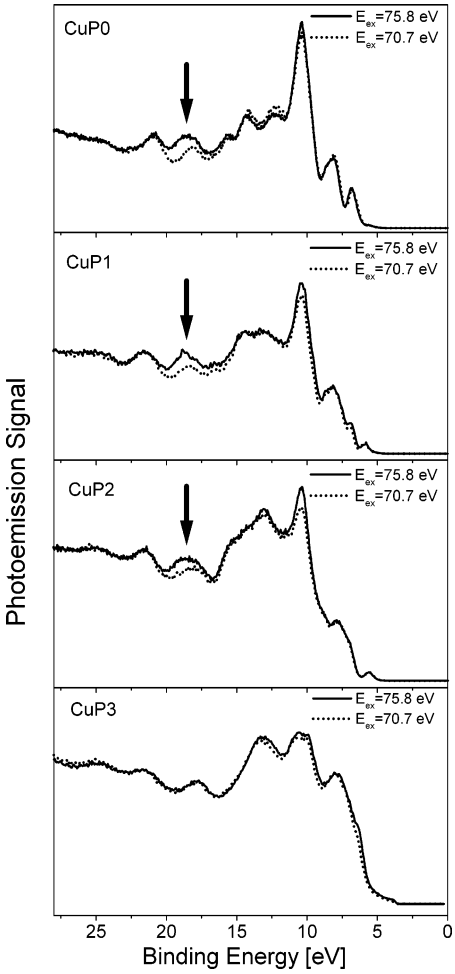

Figure 8. Photoemission spectra for thin films of the copper porphyrazine compounds, obtained with 70.7 and 75.8 eV photon energy. Arrows mark the Cu3d satellite peaks near 18 eV binding energy.

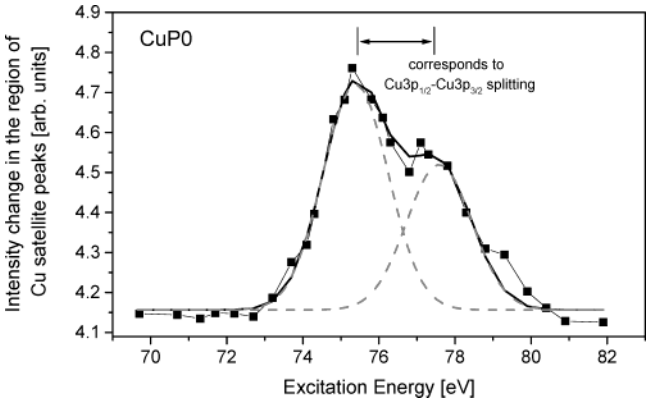

Figure 9. Intensity change in the region of the copper satellite peaks for CuP0 as a function of the excitation energy. The solid thick line represents the fit to the data assuming two Gaussians of identical widths and separated by 2.2 eV (see text).

Since the satellite enhancement involves the 3p−3d excitation, at least one hole in the 3d (namely, $Cud_{x^2-y^2}$) level must exist. Thus, the presence or absence of the satellite enhancement is an indication of an incompletely versus fully filled 3d shell, respectively. Then, the results from Figure 8 suggest that for CuPc, CuP0, CuP1, and CuP2 compounds the copper configuration in the ground state is nominally $3d^9$, whereas in the largest compound, CuP3, the copper atom would have a $3d^{10}$ formal configuration.

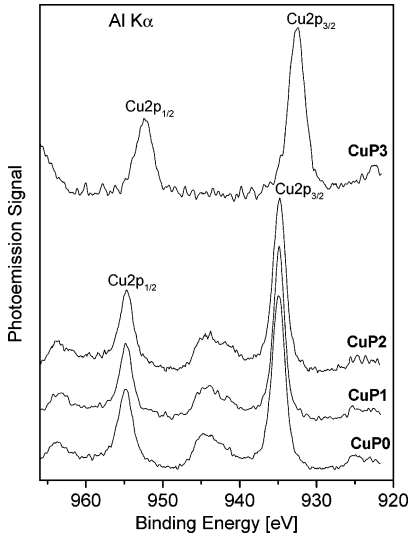

Figure 10. Cu2p X-ray photoelectron spectra for the investigated copper porphyrazines. The curves are normalized to the $Cu2p_{3/2}$ peak height and vertically displaced for clarity. See text for details.

However, in the case of CuP3, at photon energies where the 3p−4s excitation may occur for a compound with a full 3d shell, no clear resonant enhancement of any photoemission feature is observed.

3.6. XPS Measurements. Further corroboration for the initial state configuration of the central Cu atom comes from additional XPS studies using nonmonochromatized AlKα radiation. Figure 10 presents X-ray photoelectron spectra in the region of the Cu2p core levels for the four Cu−porphyrazines. From each spectrum, a linear background was subtracted. The binding energy scale was established by setting the C1s peak at a binding energy of 284.2 eV, as reported for the aromatic carbon peak of CuPc in ref 46. The weak features observed at ca. 10 eV lower binding energy relative to the $Cu2p_{3/2}$ main lines are due to the excitation of the sample by the $AlK\alpha_{3,4}$ radiation components. It is noticed that for CuP0, CuP1, and CuP2, broad satellite peaks are present on the high binding energy side of the $Cu2p_{1/2}$ and $Cu2p_{3/2}$ main lines. These type of satellites are characteristic of materials having a copper $3d^9$ configuration in the ground state.[42] The main line for each of the two split components corresponds to a charge-transfer final state in which a core hole is screened by the electron transfer from the ligand to Cu3d, being associated with the $\underline{2p}3d^{10}\underline{L}$ final state. The satellites correspond to the unscreened final state, being predominantly due to $\underline{2p}3d^9$ final configuration.[41] The binding energies for the $Cu2p_{3/2}$ main line are 934.9 ± 0.2, 934.9 ± 0.2, and 934.8 ± 0.2 eV for CuP0, CuP1, and CuP2, respectively. The satellite peaks have identical binding energies for the three compounds.

In the case of a CuP2 film, two different preparation methods were compared. Thus, XPS measurements were performed for a CuP2 film obtained by sublimation and a film prepared ex situ by the wet chemical method. Significant oxygen signal was detected in the case of the ex situ prepared film but not for the vacuum sublimed film. The N peak for the ex situ prepared film was found to shift by 0.12 eV to higher binding energy and having a shoulder as compared to the sublimed one. The Cu2p spectra showed a broadening of the main lines, a shoulder on the low binding energy side of each Cu2p main line, and a slight decrease of the ratios between satellites and main lines relative to the case of the sublimed film. The latter observations indicate the reduction of some of the central copper atoms in the molecules from the wet-prepared film, most likely due to

the interaction with the ambient atmosphere during film preparation. Yet, since the N1s and Cu2p spectra for the two films were reasonably similar, the effect of the wet chemical preparation was concluded to be minor for CuP2. On the basis of that, we also considered that the spectra of a CuP3 film prepared by the wet chemical method are likely to qualitatively reflect the properties of the original material.

The Cu2p XP spectrum of the CuP3 compound in Figure 10 shows no satellites, and one can notice that the $Cu2p_{1/2}$ and $Cu2p_{3/2}$ lines are shifted by about 2.3 eV toward lower binding energies as compared to the other molecules. The $Cu2p_{3/2}$ peak is found at 932.6 ± 0.2 eV in this case. The main lines are broader, which is attributed to the ex situ preparation. As the absence of the Cu2p satellites is generally associated with a filled 3d shell for Cu in a molecule, the present XPS results support a nominal $3d^{10}$ ground-state configuration of the central copper in the molecules of the CuP3 film.

The binding energies of the N1s core level are similar in CuP0, CuP1, and CuP2 (~398.3 ± 0.2 eV − not shown here). For CuP3, the separation between C1s and N1s peaks is by 1 eV larger than for CuP0, CuP1, or CuP2. We interpret this shift in binding energy as being due to the $Cu3d^{10}$ configuration in CuP3 (as compared to $Cu3d^9$ in the other copper porphyrazines), and we consequently attribute it to a distortion in the Cu−N bond. Actually, in the case of Cu_2O, where Cu appears as Cu^+, the binding energy of the oxygen 1s peak (oxygen is the ligand in that case) was found to be larger by roughly 1 eV than in CuO (where the Cu appears as Cu^{2+}).[42] However, the N1s peak for CuP3 was found to be much broader than for CuP0, CuP1, or CuP2. This was also observed after the CuP3 film was annealed at 250 °C. These results indicate a stronger influence of the preparation method (wet chemical) on the CuP3 compound than on the CuP2 one.

Hence, the X-ray photoemission spectra of CuP0, CuP1, and CuP2 compounds show features characteristic for a $Cu3d^9$ nominal configuration in the ground state and on the contrary, the CuP3 X-ray photoemission spectra are typical for compounds with $Cu3d^{10}$ configuration in the ground state. However, the different initial configuration for CuP3 might be well due to the ex situ preparation method for the film.

3.7. Dependence of the Satellites on Ligand Size. By comparing the XPS and UPS data for the copper porphyrazines, aspects related to the copper−nitrogen bonding might be inferred.

XPS data for CuP0, CuP1, and CuP2 reveal a slight increase of the $Cu2p_{1/2}$ and $Cu2p_{3/2}$ satellite intensities relative to those of the respective main lines as a function of ligand size. Figure 11a displays the ratio between the area of the $Cu2p_{1/2}$ satellite and the area of the $Cu2p_{1/2}$ main line, after linear background subtraction. A similar dependence was also obtained for the $Cu2p_{3/2}$ satellite/main line ratios. For a better illustration of these results, Figure 11b displays the overlapped XP spectra of CuP0 and CuP2. The increased satellite intensity for CuP2 is clearly visible.

To determine the Cu satellite-to-main line intensity ratio for the valence region, the ligand contributions had to be subtracted from the spectra. This was achieved by subtracting the contributions of the corresponding metal-free compound from each Cu−porphyrazine spectrum. The respective Cu- and metal-free porphyrazine spectra were obtained for identical experimental conditions. To account for the different background signals, in a first step a background having a linear and a Shirley[49] component was subtracted from all copper and metal-free porphyrazines spectra. The resulting spectra were then overlapped at the features of exclusive ligand character, and the metal-free compounds' curves were subtracted from the corresponding Cu−porphyrazine ones. Figure 12 shows the overlap between CuP1 and H_2P1 spectra after background subtraction and their difference signal.

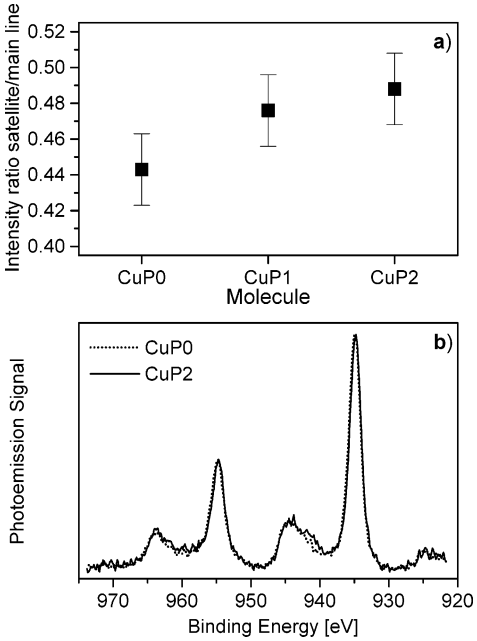

Figure 11. (a) Intensity ratio between the $Cu2p_{1/2}$ satellite and the $Cu2p_{1/2}$ main line for CuP0, CuP1, and CuP2. (b) X-ray photoelectron spectra for CuP0 and CuP2 in the region of Cu2p core levels. The satellite peaks have different intensities relative to the main lines in the two compounds.

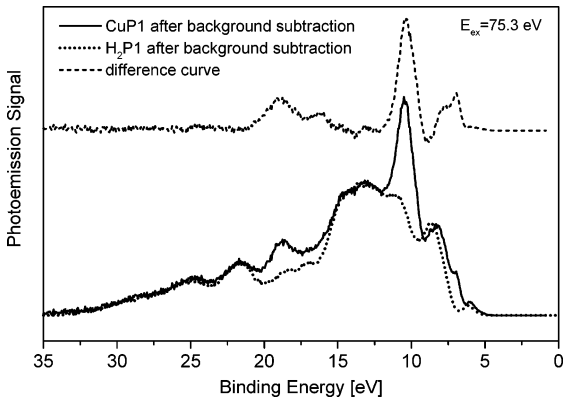

Figure 12. Overlapped CuP1 and H_2P1 spectra, both after background subtraction (bottom), and their difference curve obtained by subtracting the H_2P1 spectrum from the CuP1 one (top).

The intensities of the Cu satellite features and of the main line for a given Cu compound were calculated by integration of the difference curve at the respective positions. Generally, ligand photoemission features of the Cu and H_2 compounds overlapped reasonably well after background subtraction. However, the CuP0 and H_2P0 spectra did not always match well for all ligand features, and in such cases, the corresponding satellite/main line intensity ratios for CuP0 were overestimated. The satellite-to-main line intensity ratios for CuP1 and unsubstituted CuPc were found to be similar for identical excitation energies; hence, the *t*-butyl substitution does not affect this value.

The satellite-to-main line intensity ratios for CuP0, CuP1, and CuP2 at two off-resonant excitation energies (70.7 and 80.9 eV) and at resonant excitation energies (75.3 and 75.8 eV) are presented in Figure 13. The results were obtained by integrating

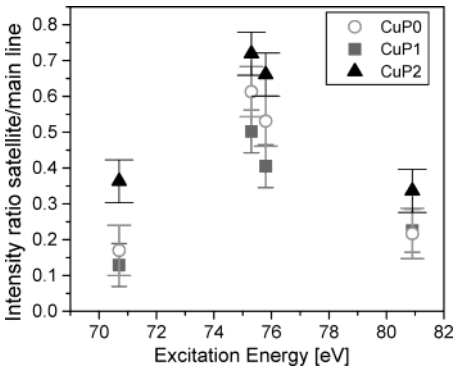

Figure 13. Intensity ratio between the satellite and the main line in the valence region for CuP0, CuP1, and CuP2 at 70.7, 75.3, 75.8, and 80.9 eV excitation energy, respectively. The results were obtained by integrating the signal of the satellite peaks at the position of band F′.

the signal of the satellite peaks at the position of band F′. These data represent average values determined after analysis of several data sets for each compound. A similar dependence was obtained by accounting for the extended satellite range (i.e., integration at the positions of bands F and F′—not shown here). The data for CuP1 and CuP2 show the same trend as found in the XPS measurements, namely, an increase of the satellite/main line intensity ratio with the ligand size. This ratio for CuP0 appears slightly larger than for CuP1. We attribute this behavior to the fact that the analysis for the CuP0 compound was more complicated; the spectra of CuP0 and H_2P0 did not overlap well at all ligand features and lead to overestimated values for satellite/main line intensity ratio.

Because the satellite corresponds to an unscreened final state and the main line corresponds to a screened final state for copper, we conclude that the ligand-to-metal charge transfer upon photoemission reduces with linear benzoannelation for this class of molecules. As pointed out in ref 45, for compounds having divalent copper the charge transfer from the ligand into a copper d orbital is larger for covalent compounds than for ionic ones. As a consequence, the ratio between the satellite and the main line intensities in the core level region is a measure of the degree of covalency or of the mixing of a covalent state with an ionic state (the ratio is small for covalent compounds and large for ionic ones).[45] Similar arguments should also hold for the valence region.

For phthalocyanines, it is known that the bonding between the central metal and the ligand is not purely ionic but significantly covalent.[4] For CuP0, CuP1, and CuP2, no shoulders were observed at the Cu2p main lines, and in addition, they have similar binding energies. This indicates that all copper atoms in the corresponding films have a nominal $3d^9$ initial configuration. Therefore, the increase of the copper satellite-to-main line intensity ratio for the Cu2p core levels and the valence region with increasing ligand size suggests that the degree of covalent mixing between Cu and pyrrole nitrogen decreases with the size of the molecule (or the ionic character of the Cu−N_p bond increases with molecular size). The increase of the ionic character of the Cu−N_p bond can be related to an increase in the electronegativity of the pyrrole nitrogens with the enlargement of the molecular size. This would be also consistent with the results published in ref 50.

Conclusions

A detailed and systematic study of the electronic structure of a special group of copper porphyrazine molecules, typically deposited on a gold single crystal, has been performed. The focus was on the interactions between the central metal and the organic ligand of varied size. The molecules were synthesized to have a gradually increasing number of benzo units attached to the pyrrole groups (linearly benzoannelated porphyrazines). Optical absorption measurements revealed that the increase of the π-electron system of the compounds, by the addition of benzo units, leads to considerable changes in the electronic structure. These changes are manifested by a strong shift of the characteristic absorption maximum to longer wavelengths.

Photoemission data show that the extension of the ligand by linear benzoannelation has two main effects on the photoemission spectra of the valence region: an intensity increase of the bands arising from the benzene units and a binding energy decrease of the leading band in the spectra (which has ligand character). Near 75 eV excitation energy, an enhancement of the copper satellite in the valence region occurs for CuP0, CuP1, and CuP2 but not for CuP3.

XPS measurements proved that the central copper atom has a $3d^9$ configuration in the ground state in CuP0, CuP1, and CuP2. In CuP3 films, the copper atom had a nominal $3d^{10}$ initial-state configuration. However, we cannot rule out that this is a consequence of the preparation method used for the CuP3 film (wet chemical instead of UHV sublimed).

We have shown that for CuP0, CuP1, and CuP2 photoemission spectra, the Cu3d main line corresponds to a screened final state, where upon ionization from one of the Cu d_{zx}, d_{yz}, d_{xy}, or d_{z^2} orbitals, charge transfer from nitrogen to the Cu$d_{x^2-y^2}$ orbital takes place. The valence-band satellite features found at higher binding energies correspond to a final state where no such ligand-to-metal charge transfer occurs upon ionization from one of the Cu d_{zx}, d_{yz}, d_{xy}, or d_{z^2} orbitals.

For CuP0, CuP1, and CuP2, an increase of the Cu2p satellite-to-main line intensity ratio with increasing ligand size was evidenced. Within the limits of error, a similar dependence was also observed for the satellite-to-main line intensity ratio in the valence region. Therefore, the ligand-to-metal charge transfer upon photoemission is concluded to be reduced with increasing ligand size/linear benzoannelation. Consequently, in this set of porphyrazines, the degree of covalent mixing between Cu and pyrrole nitrogen decreases with the size of the molecule (i.e., the ionic character of the Cu−N_p bond increases with molecular size).

In summary, the present results constitute a comprehensive data collection on the electronic structure of copper porphyrazines. By tracing the evolution of the copper satellite intensity relative to the main line for different ligand extensions, using various photon energies, information on the influence of benzoannelation on the metal−ligand interactions could be extracted. Specifically, details as to the metal-to-ligand and ligand-to-metal charge-transfer processes in Cu porphyrazine molecules could be inferred. These results are valuable with regard to the possibility of changing the electronic properties and intramolecular charge-transfer processes by controlling the extension of the π-electron system of molecules. Moreover, our data on these tailor-made molecules should be also relevant for interpreting electronic interactions in many other organometallic systems.

References and Notes

(1) Michel, S. L. J.; Hoffman, B. M.; Baum, S. M.; Barrett, A. G. M. Peripherally Functionalized Porphyrazines: Novel Metallomacrocycles with Broad, Untapped Potential. In *Progress in Inorganic Chemistry*; Karlin, K. D., Ed.; Wiley-Interscience: New York, 2001; Vol. 50, p 473.

(2) Stuzhin, P. A.; Ercolani, C. Porphyrazines with Annulated Heterocycles. In *The Porphyrin Handbook*; Kadish, K. M., Smith, K. M., Guilard, R., Eds.; Academic Press: New York, 2003; Vol. 15, p 263.

(3) Ghosh, A.; Gassman, P. G.; Almlof, J. *J. Am. Chem. Soc.* **1994**, *116*, 1932.

(4) Liao, M. S.; Scheiner, S. *J. Chem. Phys.* **2001**, *114*, 9780.

(5) Nalwa, H. S.; Hanack, M.; Pawlowski, G.; Engel, M. K. *Chem. Phys.* **1999**, *245*, 17.

(6) Reimers, J. R.; Lu, T. X.; Crossley, M. J.; Hush, N. S. *Chem. Phys. Lett.* **1996**, *256*, 353.

(7) *Phthalocyanines. Properties and Applications*; Leznoff, C. C., Lever, A. B. P., Eds.; VCH: New York, 1989; Vol. 1.

(8) *Phthalocyanines. Properties and Applications*; Leznoff, C. C., Lever, A. B. P., Eds.; VCH: New York, 1993; Vol. 3.

(9) Tomiyama, T.; Watanabe, I.; Kuwano, A.; Habiro, M.; Takane, N.; Yamada, M. *Appl. Opt.* **1995**, *34*, 8201.

(10) Ali, H.; van Lier, J. E. *Chem. Rev.* **1999**, *99*, 2379.

(11) Nalwa, H. S.; Kakuta, A.; Mukoh, A. *J. Phys. Chem.* **1993**, *97*, 1097.

(12) Hanack, M.; Dürr, K.; Lange, A.; Barcina, J. O.; Pohmer, J.; Witke, E. *Synth. Met.* **1995**, *71*, 2275.

(13) Freyer, W.; Stiel, H.; Teuchner, K.; Leupold, D. *J. Photochem. Photobiol. A* **1994**, *80*, 161.

(14) Freyer, W.; Stiel, H.; Leupold, D. *J. Inform. Rec.* **2000**, *25*, 95.

(15) Carniato, S.; Dufour, G.; Rochet, F.; Roulet, H.; Chaquin, P.; Giessnerprettre, C. *J. Electron Spectrosc. Relat. Phenom.* **1994**, *67*, 189.

(16) Liang, X. L.; Flores, S.; Ellis, D. E.; Hoffman, B. M.; Musselman, R. L. *J. Chem. Phys.* **1991**, *95*, 403.

(17) Ghosh, A.; Fitzgerald, J.; Gassman, P. G.; Almlof, J. *Inorg. Chem.* **1994**, *33*, 6057.

(18) Orti, E.; Brédas, J. L. *J. Am. Chem. Soc.* **1992**, *114*, 8669.

(19) Vilesov, F. I.; Zagrubskii, A. A.; Garbuzov, D. Z. *Sov. Phys. Solid State* **1964**, *5*, 1460.

(20) Höchst, H.; Goldmann, A.; Hüfner, S.; Malter, H. *Phys. Status Solidi B* **1976**, *76*, 559.

(21) Berkowitz, J. *J. Chem. Phys.* **1979**, *70*, 2819.

(22) Iwan, M.; Eberhardt, W.; Kalkoffen, G.; Koch, E. E.; Kunz, C. *Chem. Phys. Lett.* **1979**, *62*, 344.

(23) Tegeler, E.; Iwan, M.; Koch, E. E. *J. Electron Spectrosc. Relat. Phenom.* **1981**, *22*, 297.

(24) Lozzi, L.; Santucci, S. *Surf. Sci.* **2001**, *482*, 669.

(25) Liu, Y. Q.; Zhu, D. B.; Ge, M. F.; Qian, X. M.; Zhu, X. J.; Wang, D. X. *J. Electron Spectrosc. Relat. Phenom.* **2000**, *108*, 213.

(26) Savy, M.; Riga, J.; Verbist, J. J. *Appl. Surf. Sci.* **1989**, *35*, 454.

(27) Ottaviano, L.; Lozzi, L.; Montefusco, A.; Santucci, S. *Surf. Sci.* **1999**, *443*, 227.

(28) Ottaviano, L.; Lozzi, L.; Ramondo, F.; Picozzi, P.; Santucci, S. *J. Electron Spectrosc. Relat Phenom.* **1999**, *105*, 145.

(29) Ottaviano, L.; Lozzi, L.; Santucci, S. *Surf. Sci.* **1999**, *431*, 242.

(30) Pop, D.; Winter, B.; Freyer, W.; Hertel, I. V.; Widdra, W. *J. Phys. Chem. B* **2003**, *107*, 11643.

(31) Freyer, W.; Minh, L. Q. *Monatsh. Chem.* **1986**, *117*, 475.

(32) Kobayashi, N.; Konami, H. Molecular Orbitals and Electronic Spectra of Phthalocyanine Analogues. In *Phthalocyanines. Properties and Applications*; Leznoff, C. C., Lever, A. B. P., Eds.; VCH: New York, 1996; Vol. 4, p 345.

(33) Rosa, A.; Baerends, E. J. *Inorg. Chem.* **1994**, *33*, 584.

(34) Wen, T. C.; Tsai, C. Y. *Chem. Phys. Lett.* **1999**, *311*, 173.

(35) Berkovitch-Yellin, Z.; Ellis, D. E. *J. Am. Chem. Soc.* **1981**, *103*, 6066.

(36) Liao, M. S.; Scheiner, S. *J. Comput. Chem.* **2002**, *23*, 1391.

(37) Orti, E.; Crespo, R.; Piqueras, M. C.; Tomas, F. *J. Mater. Chem.* **1996**, *6*, 1751.

(38) Iwan, M.; Koch, E. E.; Chiang, T. C.; Eastman, D. E.; Himpsel, F.-J. *Solid State Commun.* **1980**, *34*, 57.

(39) Pop, D. Photoelectron Spectroscopy on Thin Films of Cu-, Zn-, and Metal-Free Extended Porphyrazines. Ph.D. Thesis, Freie Universität Berlin, 2003. http://www.diss.fu-berlin.de/2003/168/

(40) Grioni, M.; Goedkoop, J. B.; Schoorl, R.; de Groot, F. M. F.; Fuggle, J. C.; Schäfers, F.; Koch, E.-E.; Rossi, G.; Esteva, J.-M.; Karnatak, R. C. *Phys. Rev. B* **1989**, *39*, 1541.

(41) van der Laan, G.; Westra, C.; Haas, C.; Sawatzky, G. A. *Phys. Rev. B* **1981**, *23*, 4369.

(42) Ghijsen, J.; Tjeng, L. H.; van Elp, J.; Eskes, H.; Westerink, J.; Sawatzky, G. A.; Czyzyk, M. T. *Phys. Rev. B* **1988**, *38*, 11322.

(43) Ghijsen, J.; Tjeng, L. H.; Eskes, H.; Sawatzky, G. A.; Johnson, R. L. *Phys. Rev. B* **1990**, *42*, 2268.

(44) Tjeng, L. H.; Brookes, N. B.; Sinkovic, B. *J. Electron Spectrosc. Relat. Phenom.* **2001**, *117*, 189.

(45) Kawai, J.; Tsuboyama, S.; Ishizu, K.; Miyamura, K.; Saburi, M. *Anal. Sci.* **1994**, *10*, 853.

(46) Rochet, F.; Dufour, G.; Roulet, H.; Motta, N.; Sgarlata, A.; Piancastelli, M. N.; Decrescenzi, M. *Surf. Sci.* **1994**, *319*, 10.

(47) Hüfner, S. Charge-Excitation Final States: Satellites. In *Photoelectron Spectroscopy*; Springer-Verlag: Heidelberg, 1995; p 70.

(48) Goldoni, A.; Corradini, V.; del Pennino, U.; Sangalli, P.; Parmigiani, F.; Avila, J.; Teodorescu, C. *Europhys. Lett.* **2000**, *50*, 347.

(49) Shirley, D. A. *Phys. Rev. B* **1972**, *5*, 4709.

(50) Freyer, W.; Minh, L. Q. *J. Porphyrins Phthalocyanines* **1997**, *1*, 287.